Monitoring Body Fluids in Textiles: Combining Impedance and Thermal Principles in a Printed, Wearable, and Washable Sensor

Peer-reviewed author version

JOSE, Manoj; OUDEBROUCKX, Gilles; BORMANS, Seppe; Veske, Paula; THOELEN, Ronald & DEFERME, Wim (2021) Monitoring Body Fluids in Textiles: Combining Impedance and Thermal Principles in a Printed, Wearable, and Washable Sensor. In: ACS Sensors, 6 (3) , p. 896 -907.

DOI: 10.1021/acssensors.0c02037
Handle: http://hdl.handle.net/1942/34144

ACS SENSORS

pubs.acs.org/acssensors Article

Monitoring Body Fluids in Textiles: Combining Impedance and Thermal Principles in a Printed, Wearable, and Washable Sensor

Manoj Jose, Gilles Oudebrouckx, Seppe Bormans, Paula Veske, Ronald Thoelen, and Wim Deferme*

Cite This: https://dx.doi.org/10.1021/acssensors.0c02037 Read Online

ACCESS | Metrics & More | Article Recommendations | SI Supporting Information

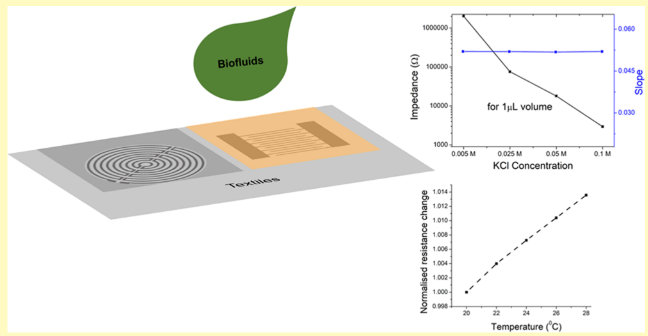

ABSTRACT: This work explores the feasibility of coupling two different techniques, the impedance and the transient plane source (TPS) principle, to quantify the moisture content and its compositional parameters simultaneously. The sensor is realized directly on textiles with the use of printing and coating technology. Impedance measurements use the fluid's electrical properties, while the TPS measurements are based on the thermal effusivity of the liquid. Impedance and TPS measurements show equal competency in measuring the fluid volume with a lowest measurable quantity of 0.5 μL, enabling ultralow volume passive measurements for sweat analysis. Both sensor principles were tested by monitoring the drying of a wet cloth and the measurements show perfect repeatability and accuracy. Nevertheless, when the biofluid property changes, the TPS sensor does not reflect this information on its readings, whereas, on the other hand, impedance can provide information on compositional changes. However, since the volume of the fluid changes simultaneously, one cannot differentiate between a volume change and a compositional change from impedance measurements alone. Therefore, we show in this work that we can apply impedance to measure the compositional properties; meanwhile, the TPS measurements accurately carry out volume measurements irrespective of the interferences from its compositional variations. To prove this, both of these techniques are applied for the quantification and composition monitoring of sweat, showing the capability to measure moisture content and compositional parameters simultaneously. TPS measurements can also be an indicator of the local temperature of the medium confined by the sensor, and it does not influence the fluid parameters. Compiling both impedance and thermal sensors in a single platform triggers smart wearable prospects of metering the liquid volume and simultaneously analyzing other compositional changes and body temperature. Finally, the repeatability and stability of the sensor readings and the washability of the device are tested. This device could be a potential sensing tool in real-life applications, such as wound monitoring and sweat analysis, and could be a promising addition toward future smart wearable sensors.

KEYWORDS: *textile, biofluid, printed, moisture content, composition analysis, sweat monitoring, ionic concentration, temperature measurement, washability*

Charles Darwin wrote in the 1800s "It is not the strongest of the species that survives, nor the most intelligent, but the one most responsive to change". Nowadays, the health care system has been transiting from physical hospitals toward virtual hospitals where the patients themselves carry miniaturized versions of medical labs, i.e., wearable sensors that do not interrupt the human being's normal life. Physical, chemical, and biological human body responses become the primary analytes for future health monitoring in medical systems. Although health-monitoring smartwatches and activity-tracking health bands have been exhibiting growing potential for commercialization, biofluid-based sensor patches are yet to be matured for health markets. Peripheral body biofluids such as sweat and wound swabs are analytes containing human body responses that assist the vital learning of the physiological and psychological aspects of human health in a noninvasive manner. Hydration monitoring,[1] perspiration analysis,[2] stress monitoring,[3] early detection of cystic fibrosis,[4] and thermal-comfort detection are some of the major health-tracking proposals of sweat volume and analyte-based wearables. McColl et al. utilized moisture-level tracking to optimize wound dressing management,[5] and many other studies report on wound exudate analysis to make effective wound-healing monitoring.[6,7] There are also reports for numerous feasibility studies employing wound discharge pH to monitor the healing progress,[8,9] and other researches have shown the exudate impedance changes as a pointer for infection detection.[10,11] The analytical studies based on the biofluids largely depend on

Received: September 30, 2020
Accepted: January 14, 2021

the quantification of biomarkers such as volume,[12,13] ionic concentration,[14−16] bacterial presence,[10,17] pH,[9,18] and similar parameters.

Most of the reported studies in the literature took advantage of monitoring the electrical properties for determining the aforementioned biomarkers, whereas these biomarkers are generally tracked individually without any cross-sensitivity in laboratory conditions. Bacterial detection in (simulated) wound exudate is conducted on a defined volume of the test liquid,[19] and the perspiration analysis assumes a uniform sweat rate. Wearable sweat analyte-monitoring studies have been reported, focusing on the sportsman's biochemical and physiological account to optimize the performance. However, recent studies emphasize the necessity of volume measurements for comprehensiveness.[20,21] Such errors can also occur during the practical measurements of pH of the biofluids.[22] Many wearable sensors in the literature have been originally designed to sense a predefined volume of the test fluid but may lose accuracy when exposed to an unknown volume. Moisture content tracking on wearable applications suffers from measurement errors due to the variations in electrical properties of the body fluids.[23−25]

To avoid the cross-sensitivity on sweat rate measurements in thermal-comfort monitoring, Sim et al. developed a watchlike device that uses expensive and high-power-consuming complex methodologies to perform accurate sweat rate sensing. This system consists of heaters, humidity sensors, actuators, and a diaphragm-enclosed frame, which are limited to be a wrist watchlike instrument and are not suitable for any other wearable textile applications mentioned before.[25] Similarly, sweat rate measurements performed with the help of microfluidic channels integrated with the heater and two thermocouples at the sides are reported elsewhere. The sweat in the channels flow through the heater, and the temperature difference between the thermocouple indicates the sweat rate.[13] There were also attempts to carry out sweat rate measurements with the help of humidity sensors. Two identical humidity sensors were arranged at a differential distance from the skin, where a gasket was used to maintain definite spacing from the skin.[26] There are also sweat collection devices built to quantify sweat loss and they use microchannels reported in previous studies.[27,28] A recent study developed a novel methodology for early detection of cystic fibrosis, and here the researchers use potentiometric measurements to monitor the sweat chloride content in the biofluid. This work also studied sweat rate measurements with the help of an additional sweat collecting device to attain error-free measurements.[15] These kinds of electrochemical potential quantifications on wearables are not affected by the fluid volume above the required threshold to perform measurements. Current approaches utilize the active stimulation of the sweat glands with exercise to produce an adequate volume of sweat (more than 10 μL) to be able to perform the analysis. This, however, is often not feasible for wearable functionalities especially for patients, infants, and elderlies. Besides, many of these sweat measurement/collecting devices use channels, pumps, and relatively complex poly(dimethylsiloxane) (PDMS)-based microfabrication strategies, the downside of which are high power consumption, long-time heating, high cost, and not being feasible to be integrated into textiles. On the other hand, laboratory-based testing applied for wearable systems often assumes a definite volume of the wound exudate or sweat rate to quantify its biomarkers. Contrarily, the moisture content (volume) measurements of the biofluids are carried out assuming identical electrical properties of the liquids, which is not always the case. Therefore, erroneous measurements are achieved, which can only be solved when both volume sensing and ionic concentration measurements are independent of each other.

The selectivity toward biomarkers, their reproducibility, and difficulties in integrating conformal fluid monitoring sensors into textiles still have bottlenecks, spanning from the sensor fabrication to sensing principles and the optimal integration of multiple techniques in a wearable platform. Conventional sensor fabrication uses glass or ceramic substrates applying microfabrication techniques, such as photolithography, sputtering, and etching, and the processing involves high-temperature curing above 300 °C.[29,30] These sensors are unconformable to the human body, and mechanical mismatch with the skin elicits motion artifacts and end-user inconvenience. Multistimulant sensible skinlike devices,[31,32] wearable human emotion monitoring patches,[3] breathable and stretchable temperature sensors,[33] thermal principle-based moisture monitoring sensors, and many more have been developed over the last few years to surpass the shortcomings of conventional systems. All of these major studies are promising ones but focus on clean room-based microfabrication of flexible devices on polyamides, PDMS, etc. However, complicated sensor fabrication steps, limited substrate selectivity, and the necessity for huge investment in the production facilities are certain disadvantages. Development of low-temperature processable functional inks and compatible high-speed printing techniques launched opportunities for mass production of conformable functionalities onto flexible substrates. Although microfabrication techniques are superior for feature size, printing opens up adaptability in terms of substrate, cost, and production speed.[34] Printing is an additive manufacturing technique that simplifies the production steps and reduces production waste. The compatibility of printing the sensors on textiles shows massive opportunities for textile-based wearable applications. A few studies on multiparameter-sensing smart bandages,[35] activity trackers,[36] and imaging modality on brassiere for cancer detection[37] have been reported. However, it still remains for printed sensors on textiles to explore in detail the wearable biophysical and biochemical measurements for health and comfort.

This article addresses the research problems related to wearable biofluid monitoring as specified before. Generally, the wearable biofluid tracking sensors encounter uncertainty between the volume of the liquid and the concentration of the ions/biological contents present in it, especially in electrical property-based sensors. When it comes to the volume-based electrical parameter-detecting moisture sensors, the accuracy in measurement is substantially affected due to the presence of ions/metabolites. Similarly, electrical property-based health-monitoring wearables are adversely affected due to the unknown volume of the body fluid. To circumvent these shortcomings, the proposed work in this article attempts to club two measurement techniques for accurate and precise quantification of biofluid and its biomarkers without disruption. Impedance-based health monitoring in wearables has been reported in previous studies.[1,38] It is a widely accepted fluid-sensing technique adopted as one of the measurement techniques in this work. Prof. Gustafsson developed the transient plane source (TPS) method in 1979, as an alternative technique to measure the thermal

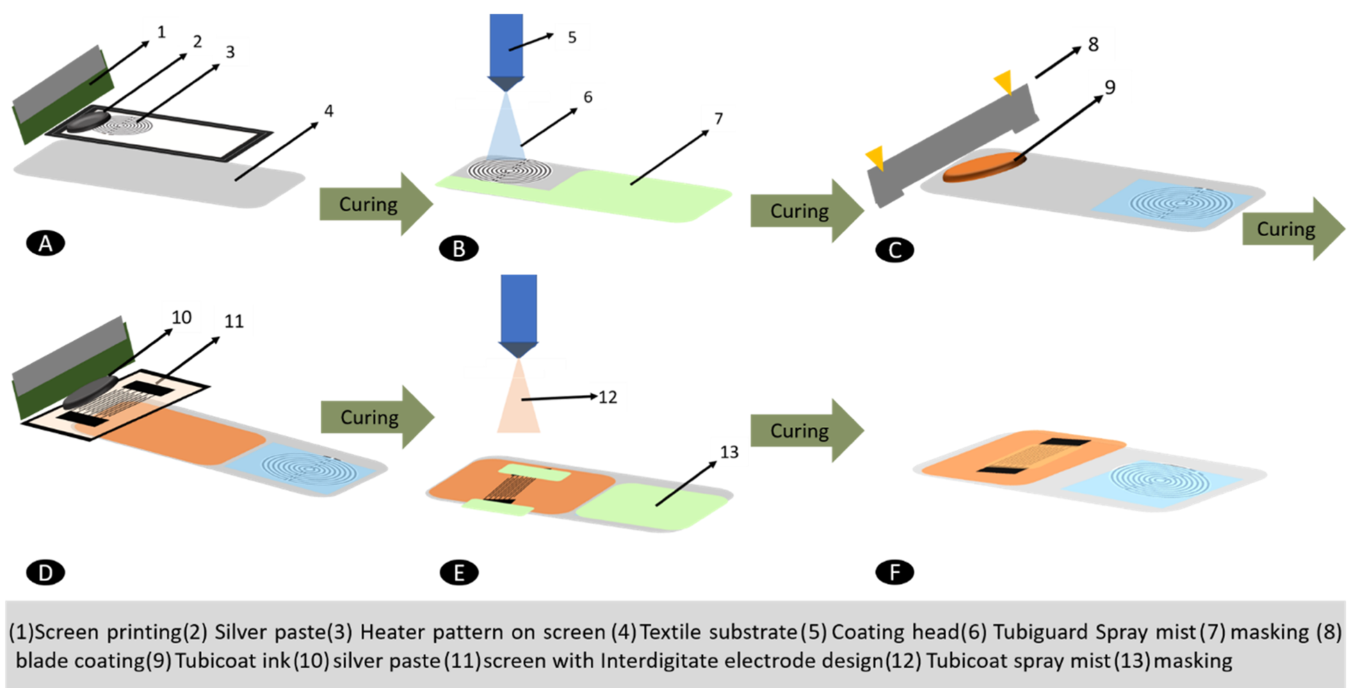

Figure 1. Sensor production flow. (A) Screen printing heater design on textiles. (B) Ultrasonic spray coating of the Tubiguard layer. (C) Blade coating Tubicoat. (D) Screen printing interdigitated electrodes (IDEs). (E) Ultrasonic spray coating of Tubicoat. (F) Final sensor on textiles.

conductivity of materials.[39] Based on this work, Schönfisch et al. presented the moisture content assessment on textiles applying the TPS method and the sensor consisted of a cleanroom microfabricated heater on polyamide foil.[40] The initial part of this article focuses on the inclusion of the TPS and impedance sensors into a single wearable textile platform. Selection of textile as the sensor substrate ensures conformability and feasibility for all range of wearable applications. As textile-compatible fabrication techniques, screen printing[41] and ultrasonic spray coating[42,43] for sensor fabrication ensured the conservation of textile wearability attributes. The final printed sensor system on textile combines the impedance and TPS technique, and both are compared for the moisture content (biofluid volume) measurement over a wide range, even with a smallest measurable quantity of 0.5 μL, which allows for passive ultralow volume sweat analysis. This work investigated the prospect to use sweat volume and composition analysis without interference. The sensor system is designed and applied for multiple biomarker detection, and it results in accurate computations without any interference. Coupled with biofluid monitoring, the human body's temperature is a highly pertinent biomarker to be tracked for wearables. Besides the fluid measurements, the TPS sensor system could manage to perform passive temperature tracking, which is also shown in this work. Finally, as the proposed sensors are fabricated on textiles, the washability of the sensors is desirable. Therefore, washing tests are performed, showing this printed sensor system's potential for long-term applications in wearables.

■ MATERIALS AND METHODS

Sensor Fabrication. The textile substrate used in this work is a polyester woven fabric (100% PES, washed and fixated, kw11401) from Concordia Textiles (Valmontheim, Belgium) with an average roughness of 6 μm. Silver paste (flexible silver paste) was purchased from Gwent group (Pontypool, U.K.), which has already been proven for its flawless performance in flexible device applications.[41] A water-based dielectric ink Tubicoat and the insulation ink Tubiguard was supplied by the CHT group, Tübingen, Germany.

TPS Moisture Sensor Fabrication. The TPS moisture sensor is directly fabricated on the textile substrate without a planarization layer. A coil heater is designed with track width and an interturn spacing of 500 μm and is screen-printed onto the textile surface (see Figure 1B). The heater design is printed using silver paste and cured at 160 °C for 20 min in a box oven to make it conductive and to remove all of the ink additives from the printed silver. The resultant heater structure has resistance in the range of 75−150 Ω at room temperature. Following this, a thin layer of Tubiguard formulation is ultrasonically spray-coated on the top of the printed silver heater. During spray coating, the heater area was left exposed and the textile's remaining area was masked with a foil. After coating, the Tubiguard layer is cured at 160 °C for 20 min in the box oven. The heater design used for sweat monitoring was smaller than the one mentioned here. The track width and spacing is set to 400 μm for the smaller heater.

Impedance Moisture Sensor Fabrication. The impedance sensor is fabricated on the textile substrate next to where the TPS sensor is printed. The textile substrate is blade-coated with a Tubicoat formulation layer to obtain a better feature size of printed electrode fingers. This sandwich architecture enhances the dielectric properties of the sensor. The coated layer was cured at 130 °C for 15 min in a box oven. Interdigitated electrodes of area 20 × 10 mm^2 are designed for the moisture sensor (see Figure 1A). The electrodes with a finger width and an interspacing of 400 μm are prepared by screen printing onto the coated side of the textile substrate, and silver paste is applied as the conductive electrode material. The printed silver electrode is cured in a box oven at 120 °C for 10 min. As a top layer for the sensor, the Tubicoat material is deposited by ultrasonic spray coating. The Tubicoat formulation is diluted to 5 wt % in water and kept in an ultrasonic bath for 5 min to make a homogeneous and fine dispersion. Ultrasonic spray coating of the diluted Tubicoat material underwent multipass coating for adequate thickness. During this step, the TPS sensor was masked with a foil to avoid the deposition of Tubicoat over it.

Agilent 4284A precision LCR meter from Hewlett Packard and PXIe-4139, a source measure unit from National Instruments, are used for the impedance and TPS sensor measurements, respectively.

https://dx.doi.org/10.1021/acssensors.0c02037
ACS Sens. XXXX, XXX, XXX−XXX

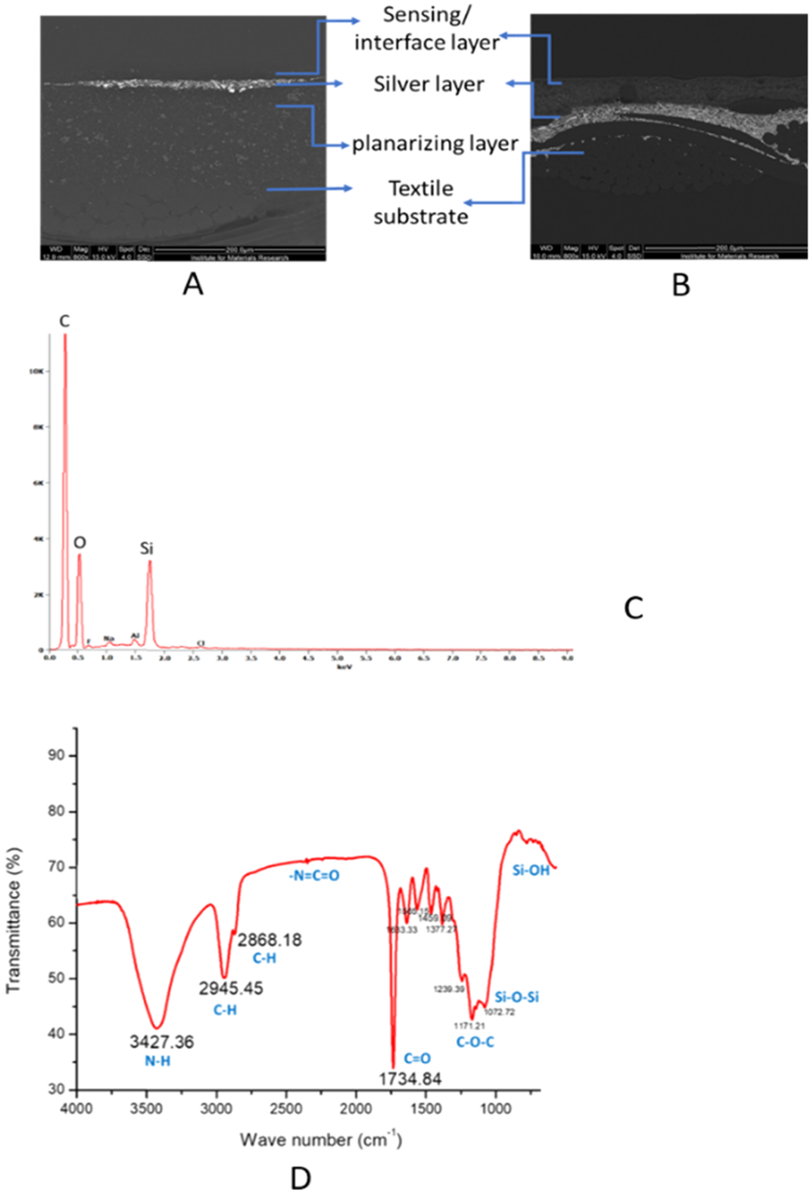

Figure 2. SEM cross section of impedance (A) and TPS sensors (B) and EDX and FTIR for the sensing layer of the impedance sensor (C and D, respectively).

Theory of Operation.[39,40,44−46] *Impedance Sensor.* The electrical impedance measurement of the moisture is based on tracking the changes in the sensor's electrical resistance and reactance when its surface comes in contact with the moisture. The proposed sensor consists of conductive interdigitated electrodes (IDEs) covered with a moisture-responsive dielectric medium. The moisture sensor's electrical model suggests that the moisture layer's intrinsic conductivity contributes to a change in the electrical resistance of the sensor.[47] Many moisture-sensing devices reported in the literature thus use fluid resistivity as the sensing parameter to quantify the fluid volume. However, the presence of moisture also produces variations in the permittivity of the dielectric sensing layer, resulting in a proportional impedance change.[48] In addition to this, the changes in the impedance occurring at the interface of the liquid and the sensing layer also add up to the total impedance, Z, and are summed up as in eq 1

$$Z = \frac{1}{2\Pi fC} + R \tag{1}$$

Here, R is the resistance, C is the capacitance, Z is the impedance, and f is the frequency.

TPS Sensor. The sensor's thermal measurements are established around a metallic heating element driven to Joule heating. As the heating element heats up, the temperature-induced resistance change is related by the renowned equation

$$R_{(t)} = R_0(1 + \alpha\Delta T) \tag{2}$$

where R_0 is the initial resistance, $R_{(t)}$ is the resistance at any instant t, and α is the temperature coefficient of resistance (TCR). The graph plotted with resistance against temperature is a straight line, and the slope is the product of α and R_0. The proposed work investigates moisture sensing using a thin-film heater, applying the transient plane source method for the measurements. The measurement is performed using a system that precisely monitors the change in temperature as the heater is triggered for a short heating pulse. When the heating sensor attains a higher temperature, it forms a thermal interface with the surroundings and the corresponding interfacial heat transfer is explained by the heat equation. The solution for the one-dimensional

https://dx.doi.org/10.1021/acssensors.0c02037
ACS Sens. XXXX, XXX, XXX−XXX

heat equation relates the change in temperature (ΔT) of the heater as a function of thermal effusivity (e) and time, as can be seen in eq 3[49]

$$\Delta T = f(e, t) \tag{3}$$

where the thermal effusivity (e) is defined as the ability of a medium to exchange heat with its surroundings and is determined as the square root of the product of volumetric heat capacity and thermal conductivity, as shown in eq 4

$$e = \sqrt{C_v \lambda} \tag{4}$$

where C_v and λ stand for volumetric heat capacity and thermal conductivity, respectively.

A short pulse of a defined power heats up the heater. The subsequent rise in temperature is in inverse proportion to the thermal effusivity of the contact medium. When the dry heater plane becomes wet, the heat energy is quickly transported from the sensor plane to the surrounding medium. As the heat energy is rapidly extracted by the water content, the sensor's rise in temperature exhibits less steepness in contrast to the sensor under dry conditions. The thermal effusivity of water is approximately 250 times higher than that of air, facilitating high sensitivity toward the presence of moisture of the sensor. The magnitude of the abovementioned effusivity of the water-content-induced temperature drop can be obtained from eq 5 that relates resistance and temperature. The variations in resistance produce changes in the applied voltage as can be seen from the equation below.[49]

$$\Delta V = I \Delta R_{(t)} \tag{5}$$

RESULTS AND DISCUSSION

Flexible and Printed Sensors on Textiles. As described in the Materials and Methods section, the impedance sensor is composed of IDEs and a sensing medium. The sensor performance in terms of sensitivity and resolution is dependent on the spacing between the interdigitates and the feature size of the electrode fingers. The interdigitated electrode spacing and feature size are limited mainly due to the printing process, substrate, and ink composition. Such sensor fabrication on textiles is often hindered due to the difficulties in fabricating IDEs on textile substrates using conventional microfabrication techniques. This work employed screen printing as a method for the deposition of IDEs on textiles. Screen printing is known for its reproducibility and good aspect ratio of the printed structures. The architecture of the sensor layer buildup is clearly observed from the scanning electron microscopy (SEM) cross section of the sensor given in Figure 2. The SEM images show that the IDEs printed on the textile substrate are rather well reproduced and the feature size of 400 μm line width is attained on the textile substrate. The presence of organic compounds and silicon in the sensing material is confirmed using energy-dispersive X-ray (EDX) spectroscopy (Figure 2C). Fourier transform infrared (FTIR) spectroscopy (Figure 2D) confirms that the sensing material consists of a polyurethane matrix and that the silicon dioxide is in the dispersed phase. Polymers, especially polyurethane, are moisture-sensitive materials and have been applied before for humidity-sensing applications.[50,51] Ceramic oxides alone serve as moisture-sensing materials, and their polymer composites improve their dielectric properties.

The intrinsic moisture conductivity, absorbed and adsorbed moisture on the polymer composite, changes the sensor's dielectric and resistive properties. The sensor's exposure to moisture results in a thin conductive moisture film on the top of the sensing layer, which contributes to impedance changes. The sensing layer's absorption phenomena lead to the emergence of the changes in interface impedance and capacitive and resistive changes on the dielectric sensing layer. The abovementioned electrical quantities contribute to the sensor impedance drop, which is proportional to the volume of the test liquid. These sensing mechanisms can be explained using the Cole−Cole plot for impedance-based moisture sensors, as shown in Figure 3A. This plot is in

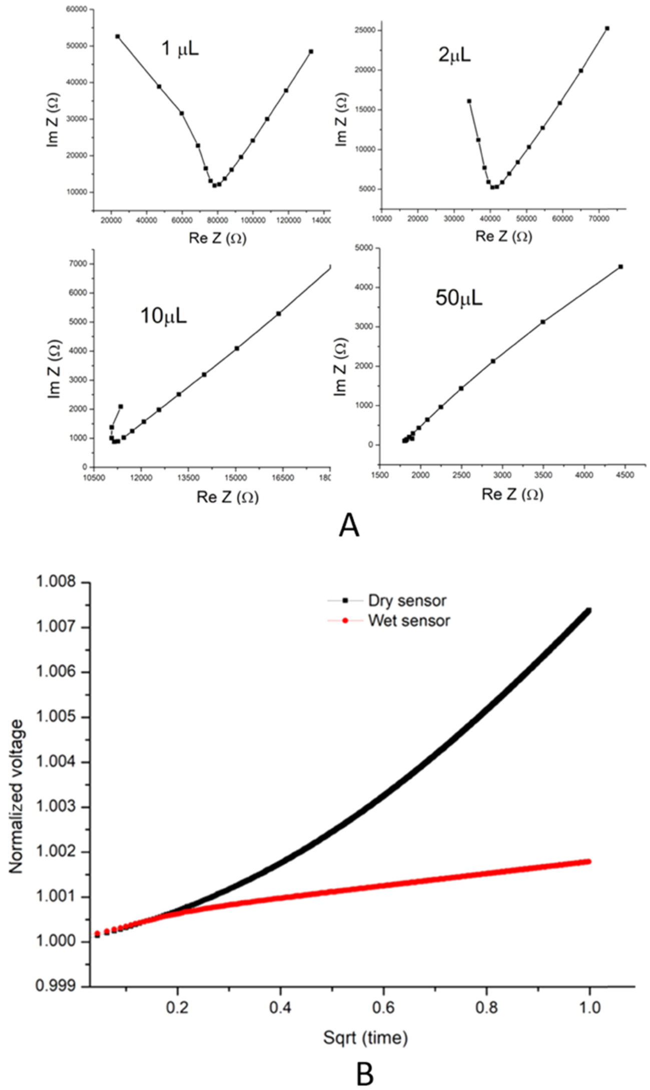

Figure 3. Cole−Cole plot for impedance sensor for different fluid volumes (A) and transient heating of a sensor at two conditions (B).

agreement with that of the sensor reported in the literature, which uses a polymer−ceramic composite layer for humidity sensing.[44] A low volume of the moisture content and high humidity levels have shown nearly the same Cole−Cole plots, paving a way for predicting the different mechanisms contributing to the impedance change.

Also, printed heaters can be used as thermal sensors for the TPS-based moisture volume measurements. The plot (Figure 3B) of the normalized voltage change vs the square root of time shows a sheer difference in the slope for wet and dry sensor surfaces. This slope is used as a parameter to quantify the water content on the surface of the sensor. Here, the TPS measurement is envisaged in such a way that spatial sensitivity is limited to the regime of the biofluid content on worn clothes

https://dx.doi.org/10.1021/acssensors.0c02037
ACS Sens. XXXX, XXX, XXX−XXX

and external ambient influences are needed to be segregated. This is achieved with the help of restricting the penetration depth of the heat pulse by setting the transient heating time (more details can be found in the Supporting Information). This work used a transient heating time of 1 s. This can be further optimized based on the end application. Prolonged transient heating leads to noise disturbances, consumes more power, and the sensor takes a long time to return to its initial condition. The printed heater has a circular coil-like structure made of conductive material. As the width of the heater coil and the spacing between them decreases, the initial resistance of the heater increases. The impact of the initial resistance on the sensitivity of the sensor is mentioned in the previous section. The heater coil feature size and the spacing between them are desired to be small to enhance the sensor sensitivity and repeatability. The cross-sectional image of the sensor given in Figure 2B shows the layer formation on the textile substrate. The printed heater sensor is encapsulated with a thin layer coating that acts as a protection layer for the conductive tracks, hindering the shunting between heater tracks during fluid testing.

Moisture Content Monitoring. This section investigates the feasibility of moisture volume measurements in textiles with the help of two different techniques. The sensors are characterized and tested for their performance in terms of work, sensitivity, precision, repeatability, and comparison of one with the other.

A moisture content measurement is performed using both the thermal- and impedance-based sensing approaches, and a comparison is made between them. In both approaches, the experiments are initiated in a dry condition. Briefly, 1−250 μL of the test liquid is dropped onto the sensor surface in discrete volumes. The impedance measurements exhibit a drop at lower frequencies, as shown in Figure 4A, whereas at higher frequencies, the impedance remains almost constant, which is as expected for resistive-capacitive circuits. As the volume of the test liquid increases, the corresponding impedance drops from a few megaohms to a few hundred ohms. Likewise, the thermal principle (TPS) was also assigned for moisture volume measurement. The printed heater is allowed to transiently heat up for 1 s, and the presence of moisture induces variations in the temperature rise of the heater. The presence of moisture segregates the heat quickly from the heater surface, and this heat transfer in turn reduces the heat buildup on the moist heater surface. The transient heating time of 1 s and the applied power are kept constant for the experiments. After every transient heating cycle, the heater remains idle for 30−100 s while it returns to its initial condition (which depends on how high the heating temperature is). The slope of the heating curve is observed to drop with increasing moisture content, as seen in Figure 4B, and this can be explained based on the section theory of operation.

The relationship of the sensor output signal as a response to the stimulus needs to be characterized, and this is known as the sensor transfer function. The impedance sensor transfer function is defined by measuring the impedance variations with moisture volume at a frequency of 100 Hz. At the same time, the TPS principle-based sensor is characterized by measuring the slope of the normalized voltage vs the square root of the time ($\sqrt{t}$) heating curve. The slope is calculated between a transient heating time of 0.5 and 0.8 $s^{0.5}$. The curve plotted between impedance and the liquid volume is best fitted to a third-order exponential decay function with an adj R^2 value of 0.999, whereas the plot of the TPS sensor is best fitted to a first-order exponential decay function with an adj R^2 value of 0.991 (Figure 5). The sensitivity of the sensor can be calculated from the derivative of the transfer functions (F1 for impedance, F2 for thermal) and are given by eqs 6 and 7.

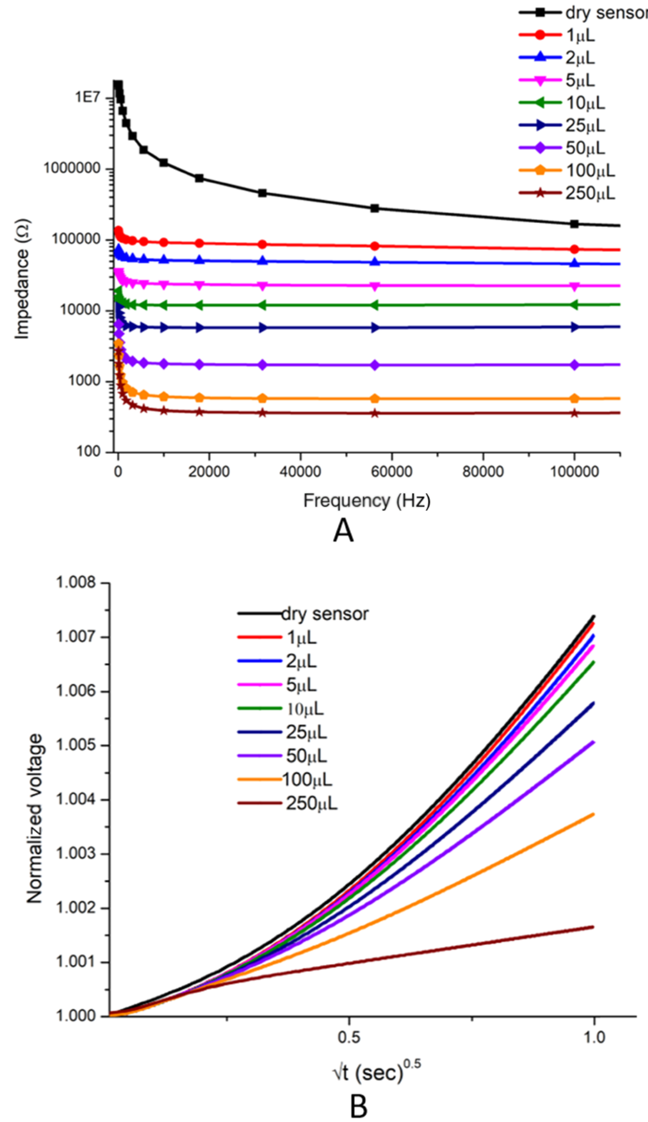

Figure 4. Moisture volume measurement from 1 to 250 μL. Impedance sensing (A) and TPS sensing (B).

$$\mathrm{d}F1/\mathrm{d}x = -11956.9\mathrm{e}^{-(x/4.6)} - 300390.6\mathrm{e}^{-(x/0.86)} - 315.38\mathrm{e}^{-(x/42.21)} \quad (6)$$

$$\mathrm{d}F2/\mathrm{d}x = 0.000598\mathrm{e}^{-(x/4.6)} \quad (7)$$

where x is the volume of the test fluid. Both the proposed impedance and TPS sensors have a least measurable volume of 1 μL for the test fluid. The impedance-based moisture sensor however has the potential to measure even smaller volumes, as is illustrated in Figure 4A, where the impedance drops a few orders of magnitude when the dry sensor becomes wet by 1 μL volume of the test liquid. The stability of the sensor readings can be evaluated by repeatedly measuring the value of the impedance for a particular volume of the test liquid. The accuracy of the sensor is evaluated from recurring readings for each test volume shown from 0 to 250 μL volume in Figure 6.

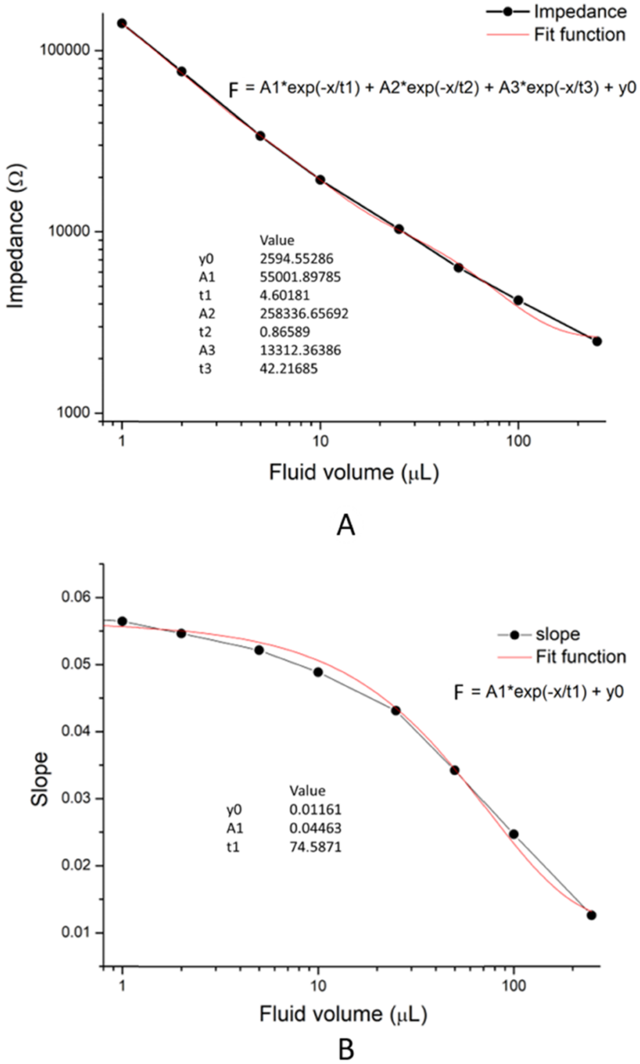

Figure 5. Moisture-sensing characteristics for the impedance sensor at 100 Hz (A) and TPS sensor (B).

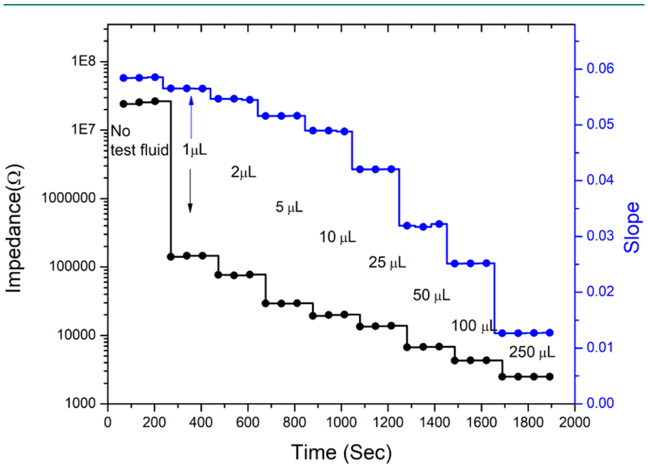

Figure 6. Impedance and TPS sensors' multiple readings for each liquid volume tested ranging from 0 to 250 μL.

Slight deviations in the sensor readings mostly arise from the dynamic spread of the liquid drop and its evaporation. The rate of evaporation increases with spreading due to the increase in the surface-to-volume ratio of the liquid drop. The accuracy of the measurements points out the necessity of another relevant attribute, which is the reproducibility of the sensor measurements in different cycles.

The reproducibility of the sensor readings over repeated measurements is also investigated. This is an inevitable feature for wearable sensors as it is directly correlated to health diagnosis. Some minor misfits are observed between the sensor readings of the repeated cycles, even at the regime of larger volumes of the test liquid. The root cause for these variations is attributed to the difference in the spreading of the liquid on the sensor surface. It is observed that both impedance and thermal measurements are influenced by the area of the liquid surface coverage. To overcome this limitation, an even surface distribution of the test fluid is a mandate. The improved wearable sensor system could be designed in such a way that the sensor is implemented to measure the volume of the liquid contained in a textile or a similar material layer coated or spread over the sensor surface, which is also shown in the next section. This modified sensor system can thus eliminate the aforementioned systemic errors, which are shown as drying of the wet textile sample.

Monitoring the Drying of a Textile Sample and the Sensors' Reproducibility. The primary goal of the proposed sensors is to measure the volume of the moisture content present in the wearables, which are wet by the secreted body fluids, and is further quantified and analyzed. The moisture volume assessment is made by monitoring the variations in the impedance and thermal measurements over a period of time where a piece of textile placed over the sensor surface is made wet and set to dry. Here, phosphate saline buffer (PBS) is applied for biofluids as it is widely recognized and used in biosensor testing.[2,11,35,52−54] Figure 7 shows the temporal evolution of (A) the impedance measurements of the sensor at a constant frequency and (B) the slope of the transient heat curve for thermal measurements. The sensor readings in the below demonstrated experiment for tracking the drying of a wet textile exhibited excellent reproducibility over repeated cycles of measurements, as is evident in the results. This feature counts as proof for the sensors' functionality to measure moisture volume, its accuracy, and reliability for real-life applications.

It can be noted here that both the sensor systems are tested and verified for over a wide input full scale, even with capacity for ultralow volumes. Both sensors are highly sensitive to moisture changes and have good repeatability irrespective of the fact that there are minor mismatches due to nonuniform wetting issues.

Synergetic Action of Impedance and Thermal (TPS) Sensors for Sweat Monitoring. As shown in the above section, both sensors show consistent and reliable sensing characteristics for volume measurements. However, wearable moisture sensors coupled with biomarker detection would be a pivotal novel functionality for comprehensive personal health management. For example, bacterial detection in wound exudate and chloride ion monitoring of sweat along with its accurate volume measurements lead to an all-inclusive fluid assessment. Figure 8 shows the sensor impedance dependency on different test liquid compositions like demi water, tap water, and phosphate buffer (PBS). The impedance readings show a completely unique sensing behavior for the test fluid where the impedance changes in response to both volume and its composition. This drives the impedance sensor into the perspectives of biofluid composition analysis to understand

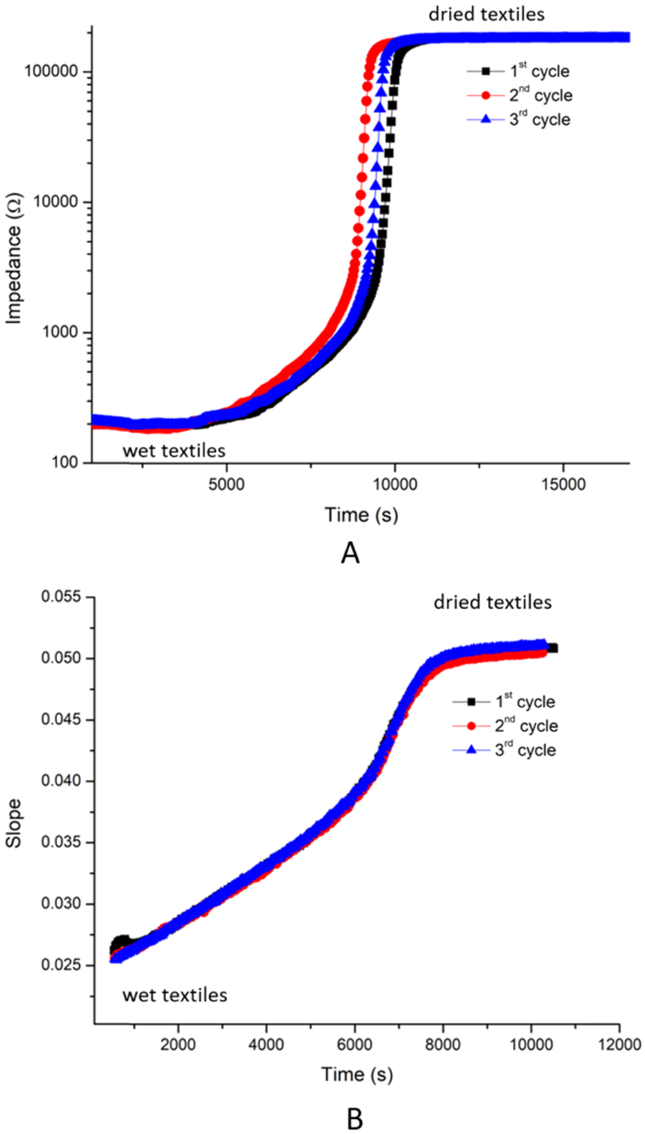

Figure 7. Drying of a wet textile monitored with impedance (A) and TPS sensors (B) shown over repeated cycles.

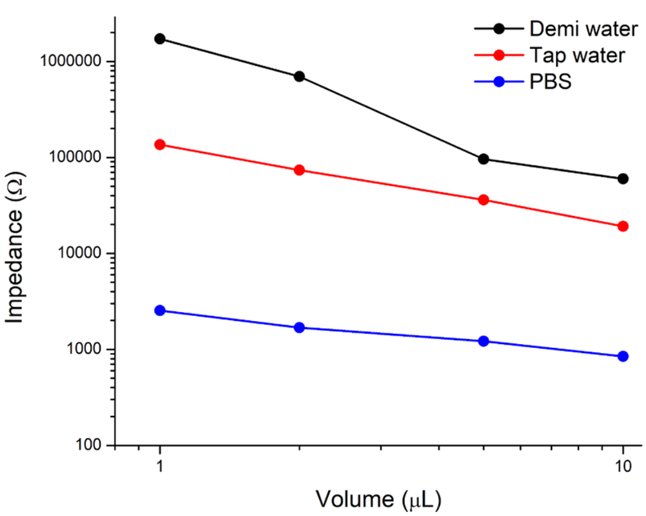

Figure 8. Impedance analysis for different fluids.

body health responses. However, this also raises a question about the uncertainty arising from the simultaneous influence of the biofluid composition and volume on the impedance measurements. As the sensor testing goes beyond the laboratory conditions from having defined volumes of the test liquid to continuously varying and unknown volumes of the biofluids, the uncertainty in impedance measurement comes into action.

The composition and volume of biofluids such as sweat vary depending on physical activities and physiological and psychological factors. In wearables, it is vital to closely monitor both the ionic composition and the volume of sweat. To address this matter of contention, the sensor system should be competent to quantify the volume of the sweat without any considerable interference from its composition and vice versa. The sweat used is prepared on the basis of European standard EN1811.[55,56] The sweat pH is adjusted to 6.5 with dilute sodium hydroxide. The sweat ionic concentration is varied in the physiologically relevant range. The concentration of sodium chloride (NaCl) is varied to different molarities, and different volumes of each are tested to see the feasibility of the sensor to be used for such applications. A few millimolar concentrations of sodium chloride ions in the test sweat produced a significant change in the impedance of the sensor (Figure 9A). Similarly, a magnificent change in the impedance is observed when the volume of the test sweat changes from 0.5 to 100 μL, whereas different fluid compositions are observed to have no significant influence on the TPS measurements of the sweat (Figure 9B). Relative to previous experiments, a more compact heater is used for the sweat-monitoring experiments. Smaller and closer tracks are used for the sweat experiments to reduce the errors from nonuniform heating. Minor misfits in the TPS readings of different concentrations, especially at higher volumes, are due to the difference in the fluid dropping and its spreading. To prove this, the sensor is tested with different concentrations of sweat in equal volumes and is dropped on a thin tissue placed on the heater surface. There was no difference observed, and all of the readings were identical (Supporting Information, Figure S-2). Compiling both impedance and TPS sensors in a single platform develops more accurate and smart wearable prospects of metering liquid volume and the simultaneous analysis of other electrical properties. The proposed sensor platform has a sensitivity to respond to a fluid volume of 0.5 μL or possibly less. Therefore, the synergistic operation of the two sensors in a combined platform enables the impedance sensor to track any compositional changes, such as ionic composition, in the sweat and the thermal sensor to determine their volume.

Temperature Monitoring as a Complementary Functionality. Temperature variations of the body or a specific body part guide disease diagnosis, activity tracking, and infection detection. This is considered one of the most important biomarkers for wearables. Metals have a positive temperature coefficient of resistance (TCR), and their resistance changes based on the temperature and its TCR. Wearable temperature sensors employing metal-coil-like structures have shown good sensitivity and accuracy.[57] The printed silver structures in this work exhibit a TCR of 0.001628, which is comparable to previously reported values.[58] The heater structure's initial resistance is proportional to the temperature of its medium, and Figure 10A indicates that the resistance increases in proportion to the temperature of the sensor-enclosed oven. Figure 10A shows that the sensor has a

https://dx.doi.org/10.1021/acssensors.0c02037
ACS Sens. XXXX, XXX, XXX−XXX

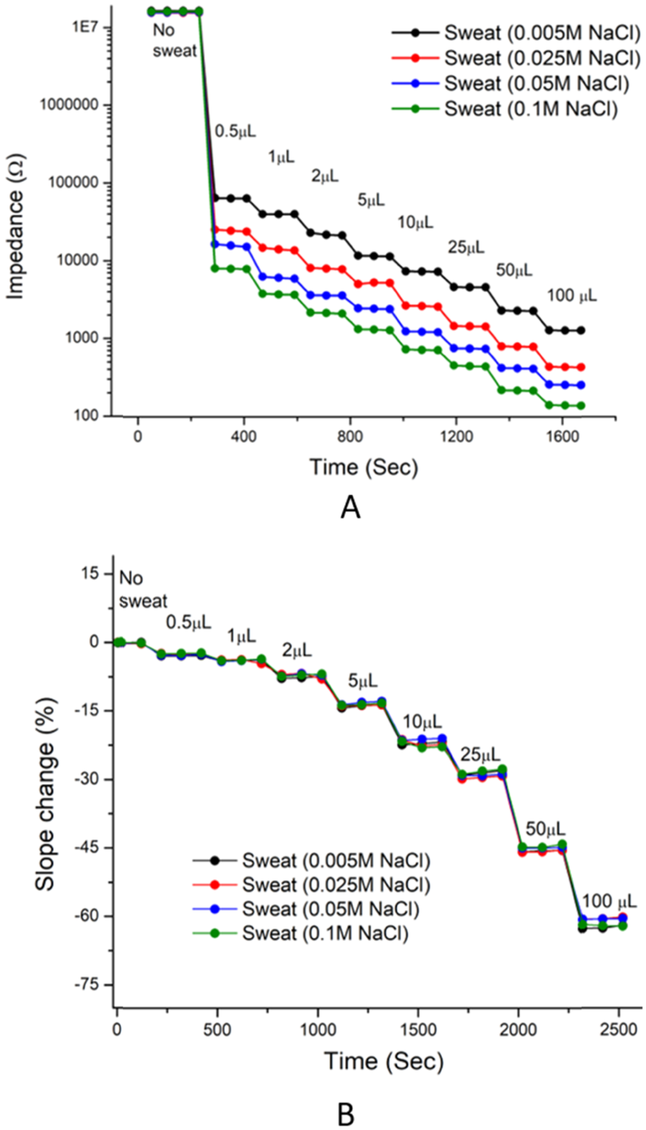

Figure 9. Experimental results of sweat monitoring. The response to volume and NaCl concentrations in sweat tested with the impedance sensor (A) and the TPS sensor (B). The impedance measurement is affected by both the NaCl concentration and the moisture content, whereas the thermal measurement is only influenced by the moisture content.

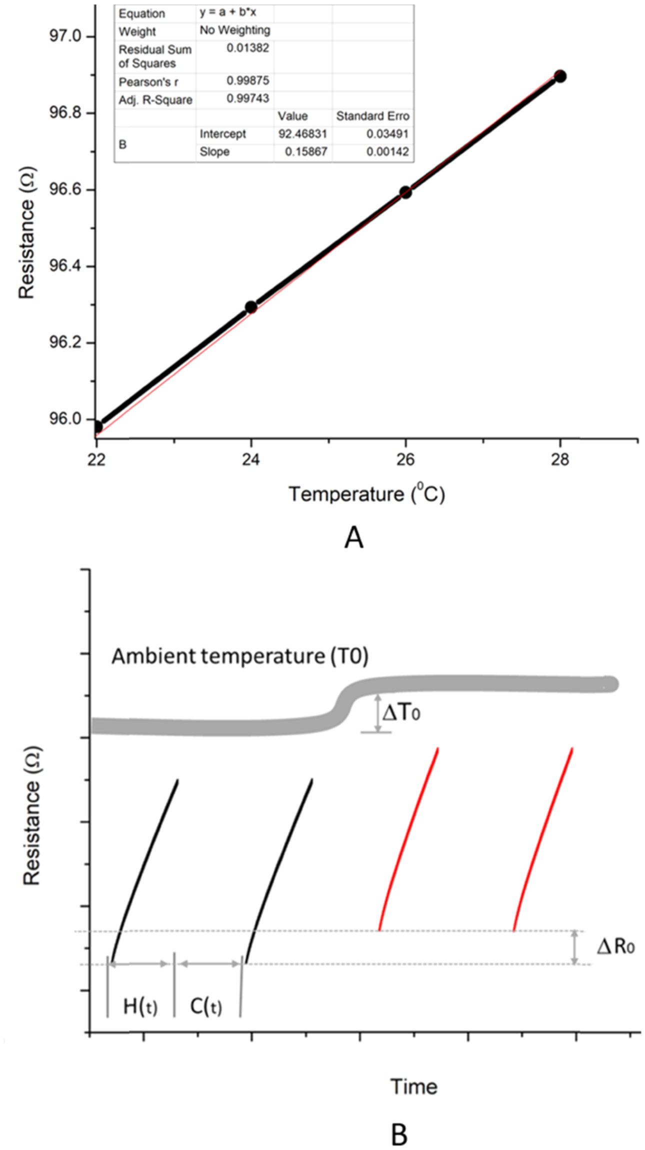

Figure 10. Resistance reading of the sensor inside an oven with the help of a multimeter, where the box oven temperature is set to vary from 22 to 28 °C (A) and illustration of TPS measurements while ambient temperature varies over time (B).

sensitivity of 0.158 Ω/°C and excellent linear transfer function characteristics. As illustrated in Figure 10B, for the TPS measurement, $H_{(t)}$ represents the duration for which a transient heat pulse is applied and $C_{(t)}$ is the cooling time where $C_{(t)} \gg H_{(t)}$. The initial resistance (R_0) of the heater at the time of applying the heat pulse is proportional to the ambient temperature (T_0). Therefore, the difference in the initial resistances of the heater measured at heat pulses indicates sensor medium-temperature variations.[59] Thus, the TPS measurement mode can be beneficially exploited to estimate an additional functionality, namely, the monitoring of the body temperature, if the body is cohesive enough to the sensor. Body fluid volume, electrical properties, and temperature measurements together pave the way for a synergic effect applicable for a myriad of wearable entreaties. Such synergetic action of the textile sensor patch could address the possibility of a smart bandage for wound monitoring. The wound exudate detection could help with the wound dressing removal and redressing, reducing the chances of infections. Infections, however, need to be detected at the earliest and wound exudate bacterial growth can be identified with impedance spectra analysis.[60,61] In conjunction with this, the temperature measurements at the wound site could guide health practitioners about the wound-healing progress.[62−64] Similarly, it is a highly germane model for sportswear to have a temperature indicator along with the sweat rate and sweat analysis.[2,59]

Washability of the Sensor. The washability of the wearable sensor is a vital aspect that makes the sensor system applicable in real-life scenarios. The sensor design architecture and material selection are crucial for the withstandability of the sensor during washing cycles. The impedance sensor is designed in such a way that the interdigitated electrodes are sandwiched in between the sensing layer medium. The sensing layer is based on polyurethane, which is compatible with

https://dx.doi.org/10.1021/acssensors.0c02037
ACS Sens. XXXX, XXX, XXX−XXX

washing. The TPS sensor buildup is made in a way that the top face of the heater structure is spray coated with Tubiguard, to form a nonabsorbent layer.

Additionally, a few TPS sensors are also fabricated with both sides of the sensor having Tubiguard layers. The washing tests are conducted based on the ISO 6330 standards, where each washing cycle is carried out at 40 °C and has a duration of 70 min each. Every sensor undergoes five such washing cycles. Washability results in Figure 11A show almost identical

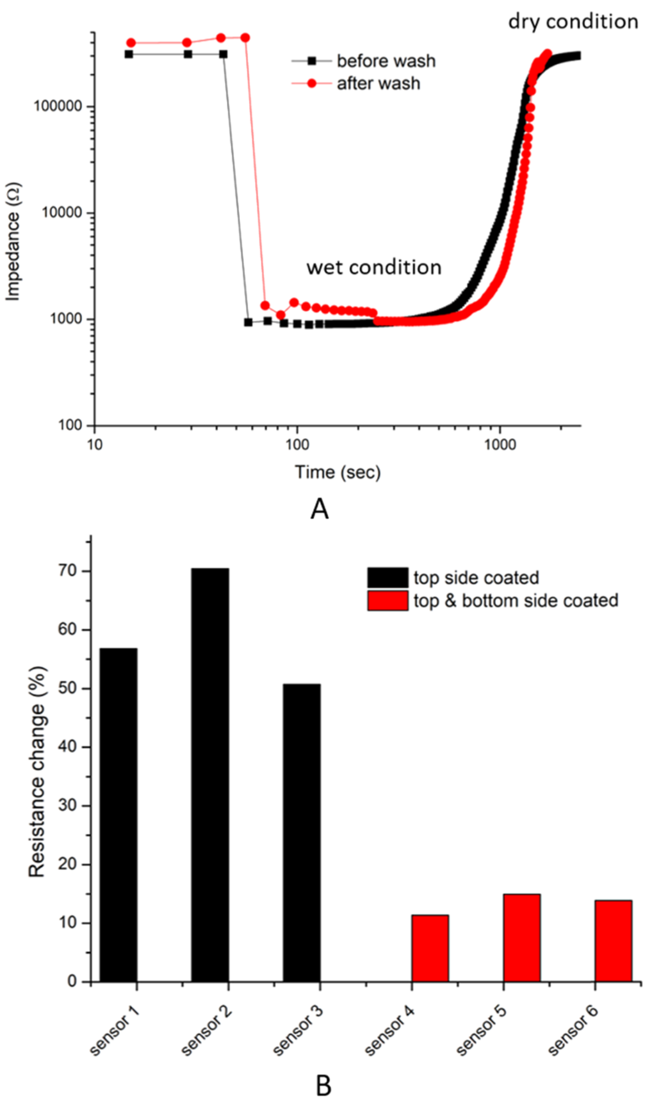

Figure 11. Impedance sensor monitoring the drying of a paper tissue before and after five washing cycles (A) and resistance change of the heater structures compared before and after washing cycles (B).

responses for the impedance measurements of the sensor before and after performing the washing tests. However, there is a slight offset that is supposed to arise from minor damages that occurred during washing, which can be addressed by increasing the thickness of the dielectric layer and adding cross linking-agents to this polymeric ink. Heaters having encapsulation layers on both sides show better performance after washing tests than those with the protective coating only on one side, as shown in Figure 11B.

■ CONCLUSIONS AND FUTURE STUDIES

In this article, an approach for a wearable biofluid monitoring system is described, combining two concurrent principles for the first time to the best of our knowledge. The article emphasizes the development of wearable techniques to carry out precise quantification of peripheral body biofluid and its biomarkers in a nonintrusive manner. Wearable sensors based on electrical parameters often suffer from cross-sensitivity of different biomarkers. This work applies two different measurement techniques: one based on electrical impedance and the other, the TPS principle, on thermal properties, combined for a comprehensive independent sensing node. The sensor system demonstrates consistent and repeatable moisture volume measurements and is also deployed to monitor the drying of wet textiles. The sensor system demonstrates the smallest measurable volume of 0.5 μL sweat, which assures the method to be promising for health monitoring. Along with volume, the sweat's compositional variations also induced changes in the impedance readings. The TPS sensor measures the volume of sweat accurately without any interference from the compositional variations. The sweat solution volume was varied with simultaneous variation in the NaCl concentration over a range of 0.005−0.1 M, and the proposed sensor system accurately tracked and measured both without any disruption. The sensor system is conceived such that it can work reciprocally toward better wearable applications.

The printed sensors on textiles incorporating this dual-sensing technique exclusively address some of the critical challenges in terms of the selectivity of biomarkers, moisture content measurement, wearability, and economic viability. Additionally, the TPS measurement system possesses the capacity to track the temperature of the medium and the textile sensor with a sensitivity of 0.158 Ω/°C. Besides the possibilities toward biofluid volume measurement, biomarker detection, and passive body temperature measurement, this work also accounts for promising results toward washing compatibility. The selection of the right materials and smart device engineering ensure the sensor's withstandability during washing and provide a promising feature. As most of the research articles focusing on wearable sensors utilize flexible foil as the substrate, this work ensures the direct fabrication of sensors on textiles. Screen printing and ultrasonic spray coating were applied to deposit different material formulations, and this enables the mass production of the conformable sensors at a reduced cost.

The developed dual sensor system can be worthwhile in real-life applications such as smart wound dressings, wearable health bands, and sports wearables. To address such end-application requirements, the sensor system needs to be ready for on-body measurements. In future studies, the authors would address body measurements where the sensors also need to be integrated together with a wearable readout system. Depending on the end-application, the sensor buildup architecture may change from side-by-side placement to a stack type. Additionally, for the TPS sensor, transient heating needs to be optimized in such a way that it measures only the moisture in textiles and does not get influenced by that from the human body. The sensor system needs considerations in its design and material selection in such a way that the errors that could be induced by body movements and other variabilities need to be kept as minimal as possible. Similarly, the experimental results also show the possibilities of the sensor system to handle volumes even less than 0.5 μL. Future studies must also check the viability to test even lower volumes by improving the printing line-width resolution that could make the heater coil and the electrode fingers even closer and thinner. This helps to get better sensitivity and repeatability of the sensor measurements. In addition, it would be beneficial if the sensor interface layer to fluids has a more efficient wetting behavior, which could be made possible with a thin hydrophilic coating or by integrating a textile layer on the sensor surface. This would add a more interesting perspective for more accurate and repeatable measurements. To conclude, this work demonstrated an innovative approach for the accurate analysis of human body fluids in wearable textiles and can progressively evolve as a step forward in smart wound monitoring and sweat analysis applications.

ASSOCIATED CONTENT

Supporting Information

The Supporting Information is available free of charge at https://pubs.acs.org/doi/10.1021/acssensors.0c02037.

Description and explanation of TPS sensor's transient heating time selection; transient heating curve; and TPS measurements of sweat with different ionic concentrations tested on thin tissue (PDF)

AUTHOR INFORMATION

Corresponding Author

Wim Deferme − *Hasselt University, Institute for Materials Research (IMO-IMOMEC) 1, 3590 Diepenbeek, Belgium; IMEC, Division IMOMEC, B-3590 Diepenbeek, Belgium;* orcid.org/0000-0002-8982-959X; Email: wim.deferme@uhasselt.be

Authors

Manoj Jose − *Hasselt University, Institute for Materials Research (IMO-IMOMEC) 1, 3590 Diepenbeek, Belgium; IMEC, Division IMOMEC, B-3590 Diepenbeek, Belgium;* orcid.org/0000-0003-1635-1131

Gilles Oudebrouckx − *Hasselt University, Institute for Materials Research (IMO-IMOMEC) 1, 3590 Diepenbeek, Belgium; IMEC, Division IMOMEC, B-3590 Diepenbeek, Belgium;* orcid.org/0000-0001-6278-3547

Seppe Bormans − *Hasselt University, Institute for Materials Research (IMO-IMOMEC) 1, 3590 Diepenbeek, Belgium; IMEC, Division IMOMEC, B-3590 Diepenbeek, Belgium*

Paula Veske − *Centre for Microsystems Technology (CMST), IMEC and Ghent University, 9052 Gent, Belgium*

Ronald Thoelen − *Hasselt University, Institute for Materials Research (IMO-IMOMEC) 1, 3590 Diepenbeek, Belgium; IMEC, Division IMOMEC, B-3590 Diepenbeek, Belgium*

Complete contact information is available at: https://pubs.acs.org/10.1021/acssensors.0c02037

Notes

The authors declare no competing financial interest.

REFERENCES

(1) Yao, S.; Myers, A.; Malhotra, A.; Lin, F.; Bozkurt, A.; Muth, J. F.; Zhu, Y. A Wearable Hydration Sensor with Conformal Nanowire Electrodes. *Adv. Healthcare Mater.* **2017**, *6*, No. 1601159.

(2) Gao, W.; Emaminejad, S.; Nyein, H. Y. Y.; Challa, S.; Chen, K.; Peck, A.; Fahad, H. M.; Ota, H.; Shiraki, H.; Kiriya, D.; Lien, D.-H.; Brooks, G. A.; Davis, R. W.; Javey, A. Fully integrated wearable sensor arrays for multiplexed in situ perspiration analysis. *Nature* **2016**, *529*, 509−514.

(3) Yoon, S.; Sim, J.; Cho, Y.-H. A Flexible and Wearable Human Stress Monitoring Patch. *Sci. Rep.* **2016**, *6*, No. 23468.

(4) Morello, R.; Capua, C. D.; Lugarà, M.; Lay-Ekuakille, A.; Griffo, G.; Vergallo, P. In *Design of a Wearable Sweat Sensor for Diagnosing Cystic Fibrosis in Children*, 2013 IEEE International Symposium on Medical Measurements and Applications (MeMeA), 4−5 May 2013; pp 268−273.

(5) McColl, D.; Cartlidge, B.; Connolly, P. Real-time monitoring of moisture levels in wound dressings in vitro: An experimental study. *Int. J. Surg.* **2007**, *5*, 316−322.

(6) Ochoa, M.; Rahimi, R.; Ziaie, B. Flexible Sensors for Chronic Wound Management. *IEEE Rev. Biomed. Eng.* **2014**, *7*, 73−86.

(7) Brown, M. S.; Ashley, B.; Koh, A. Wearable Technology for Chronic Wound Monitoring: Current Dressings, Advancements, and Future Prospects. *Front. Bioeng. Biotechnol.* **2018**, *6*, No. 47.

(8) Sharp, D. Printed composite electrodes for in-situ wound pH monitoring. *Biosens. Bioelectron.* **2013**, *50*, 399−405.

(9) Qin, M.; Guo, H.; Dai, Z.; Yan, X.; Ning, X. Advances in flexible and wearable pH sensors for wound healing monitoring. *J. Semicond.* **2019**, *40*, No. 111607.

(10) Farrow, M. J.; Hunter, I. S.; Connolly, P. Developing a real time sensing system to monitor bacteria in wound dressings. *Biosensors* **2012**, *2*, 171−188.

(11) Ciani, I.; Schulze, H.; Corrigan, D. K.; Henihan, G.; Giraud, G.; Terry, J. G.; Walton, A. J.; Pethig, R.; Ghazal, P.; Crain, J.; Campbell, C. J.; Bachmann, T. T.; Mount, A. R. Development of immunosensors for direct detection of three wound infection biomarkers at point of care using electrochemical impedance spectroscopy. *Biosens. Bioelectron.* **2012**, *31*, 413−418.

(12) Milne, S. D.; Seoudi, I.; Al Hamad, H.; Talal, T. K.; Anoop, A. A.; Allahverdi, N.; Zakaria, Z.; Menzies, R.; Connolly, P. A wearable wound moisture sensor as an indicator for wound dressing change: an observational study of wound moisture and status. *Int. Wound J.* **2016**, *13*, 1309−1314.

(13) Brueck, A.; Iftekhar, T.; Stannard, A. B.; Yelamarthi, K.; Kaya, T. A Real-Time Wireless Sweat Rate Measurement System for Physical Activity Monitoring. *Sensors* **2018**, *18*, No. 533.

(14) Chung, M.; Fortunato, G.; Radacsi, N. Wearable flexible sweat sensors for healthcare monitoring: a review. *J. R. Soc., Interface* **2019**, *16*, No. 20190217.

(15) Choi, D.-H.; Kitchen, G. B.; Jennings, M. T.; Cutting, G. R.; Searson, P. C. Out-of-clinic measurement of sweat chloride using a wearable sensor during low-intensity exercise. *npj Digital Med.* **2020**, *3*, No. 49.

(16) He, W.; Wang, C.; Wang, H.; Jian, M.; Lu, W.; Liang, X.; Zhang, X.; Yang, F.; Zhang, Y. Integrated textile sensor patch for real-time and multiplex sweat analysis. *Sci. Adv.* **2019**, *5*, No. eaax0649.

(17) Ward, A. C.; Hannah, A. J.; Kendrick, S. L.; Tucker, N. P.; MacGregor, G.; Connolly, P. Identification and characterisation of *Staphylococcus aureus* on low cost screen printed carbon electrodes using impedance spectroscopy. *Biosens. Bioelectron.* **2018**, *110*, 65−70.

(18) Manjakkal, L.; Dervin, S.; Dahiya, R. Flexible potentiometric pH sensors for wearable systems. *RSC Adv.* **2020**, *10*, 8594−8617.

(19) Miller, C.; Stiglich, M.; Livingstone, M.; Gilmore, J. Impedance-Based Biosensing of Pseudomonas putida via Solution Blow Spun PLA: MWCNT Composite Nanofibers. *Micromachines* **2019**, *10*, No. 876.

(20) Seshadri, D. R.; Li, R. T.; Voos, J. E.; Rowbottom, J. R.; Alfes, C. M.; Zorman, C. A.; Drummond, C. K. Wearable sensors for monitoring the physiological and biochemical profile of the athlete. *npj Digit. Med.* **2019**, *2*, No. 72.

(21) Heikenfeld, J.; Jajack, A.; Rogers, J.; Gutruf, P.; Tian, L.; Pan, T.; Li, R.; Khine, M.; Kim, J.; Wang, J.; Kim, J. Wearable sensors: modalities, challenges, and prospects. *Lab Chip* **2018**, *18*, 217−248.

(22) Farooqui, M. F.; Shamim, A. Low Cost Inkjet Printed Smart Bandage for Wireless Monitoring of Chronic Wounds. *Sci. Rep.* **2016**, *6*, No. 28949.

https://dx.doi.org/10.1021/acssensors.0c02037
ACS Sens. XXXX, XXX, XXX−XXX

(23) Kubiak, P.; Lesnikowski, J.; Gniotek, K. Textile Sweat Sensor for Underwear Convenience Measurement. *Fibres Text. East. Eur.* **2016**, *24*, 151−155.

(24) Amano, T.; Gerrett, N.; Inoue, Y.; Nishiyasu, T.; Havenith, G.; Kondo, N. Determination of the maximum rate of eccrine sweat glands' ion reabsorption using the galvanic skin conductance to local sweat rate relationship. *Eur. J. Appl. Physiol.* **2016**, *116*, 281−290.

(25) Sim, J. K.; Yoon, S.; Cho, Y.-H. Wearable Sweat Rate Sensors for Human Thermal Comfort Monitoring. *Sci. Rep.* **2018**, *8*, No. 1181.

(26) Salvo, P.; Francesco, F. D.; Costanzo, D.; Ferrari, C.; Trivella, M. G.; Rossi, D. D. A Wearable Sensor for Measuring Sweat Rate. *IEEE Sens. J.* **2010**, *10*, 1557−1558.

(27) Jain, V.; Ochoa, M.; Jiang, H.; Rahimi, R.; Ziaie, B. A mass-customizable dermal patch with discrete colorimetric indicators for personalized sweat rate quantification. *Microsyst. Nanoeng.* **2019**, *5*, No. 29.

(28) Reeder, J. T.; Choi, J.; Xue, Y.; Gutruf, P.; Hanson, J.; Liu, M.; Ray, T.; Bandodkar, A. J.; Avila, R.; Xia, W.; Krishnan, S.; Xu, S.; Barnes, K.; Pahnke, M.; Ghaffari, R.; Huang, Y.; Rogers, J. A. Waterproof, electronics-enabled, epidermal microfluidic devices for sweat collection, biomarker analysis, and thermography in aquatic settings. *Sci. Adv.* **2019**, *5*, No. eaau6356.

(29) Hierlemann, A.; Brand, O.; Hagleitner, C.; Baltes, H. Microfabrication techniques for chemical/biosensors. *Proc. IEEE* **2003**, *91*, 839−863.

(30) Betancourt, T.; Brannon-Peppas, L. Micro- and nanofabrication methods in nanotechnological medical and pharmaceutical devices. *Int. J. Nanomed.* **2006**, *1*, 483−495.

(31) Park, J.; Lee, Y.; Hong, J.; Lee, Y.; Ha, M.; Jung, Y.; Lim, H.; Kim, S. Y.; Ko, H. Tactile-Direction-Sensitive and Stretchable Electronic Skins Based on Human-Skin-Inspired Interlocked Microstructures. *ACS Nano* **2014**, *8*, 12020−12029.

(32) Zhang, F.; Zang, Y.; Huang, D.; Di, C.-a.; Zhu, D. Flexible and self-powered temperature−pressure dual-parameter sensors using microstructure-frame-supported organic thermoelectric materials. *Nat. Commun.* **2015**, *6*, No. 8356.

(33) Chen, Y.; Lu, B.; Chen, Y.; Feng, X. Breathable and Stretchable Temperature Sensors Inspired by Skin. *Sci. Rep.* **2015**, *5*, No. 11505.

(34) Sreenilayam, S. P.; Ahad, I. U.; Nicolosi, V.; Acinas Garzon, V.; Brabazon, D. Advanced materials of printed wearables for physiological parameter monitoring. *Mater. Today* **2020**, *32*, 147−177.

(35) Pal, A.; Goswami, D.; Cuellar, H. E.; Castro, B.; Kuang, S.; Martinez, R. V. Early detection and monitoring of chronic wounds using low-cost, omniphobic paper-based smart bandages. *Biosens. Bioelectron.* **2018**, *117*, 696−705.

(36) Krykpayev, B.; Farooqui, M. F.; Bilal, R. M.; Vaseem, M.; Shamim, A. A wearable tracking device inkjet-printed on textile. *Microelectron. J.* **2017**, *65*, 40−48.

(37) Hong, S.; Lee, K.; Ha, U.; Kim, H.; Lee, Y.; Kim, Y.; Yoo, H. A 4.9 mΩ-Sensitivity Mobile Electrical Impedance Tomography IC for Early Breast-Cancer Detection System. *IEEE J. Solid-State Circuits* **2015**, *50*, 245−257.

(38) Ganguly, A.; Prasad, S. Passively Addressable Ultra-Low Volume Sweat Chloride Sensor. *Sensors* **2019**, *19*, No. 4590.

(39) Gustafsson, S. E. Transient plane source techniques for thermal conductivity and thermal diffusivity measurements of solid materials. *Rev. Sci. Instrum.* **1991**, *62*, 797−804.

(40) Schönfisch, D.; Göddel, M.; Blinn, J.; Heyde, C.; Schlarb, H.; Deferme, W.; Picard, A. New Type of Thermal Moisture Sensor for in-Textile Measurements. *Phys. Status Solidi (a)* **2019**, *216*, No. 1800765.

(41) Verboven, I.; Stryckers, J.; Mecnika, V.; Vandevenne, G.; Jose, M.; Deferme, W. Printing Smart Designs of Light Emitting Devices with Maintained Textile Properties. *Materials* **2018**, *11*, No. 290.

(42) Samanta, A.; Bordes, R. Conductive textiles prepared by spray coating of water-based graphene dispersions. *RSC Adv.* **2020**, *10*, 2396−2403.

(43) Khattab, T. A.; Rehan, M.; Hamdy, Y.; Shaheen, T. I. Facile Development of Photoluminescent Textile Fabric via Spray Coating of Eu(II)-Doped Strontium Aluminate. *Ind. Eng. Chem. Res.* **2018**, *57*, 11483−11492.

(44) Wang, J.; Lin, Q.; Zhou, R.; Xu, B. Humidity sensors based on composite material of nano-BaTiO3 and polymer RMX. *Sens. Actuators, B* **2002**, *81*, 248−253.

(45) Farahani, H.; Wagiran, R.; Hamidon, M. N. Humidity Sensors Principle, Mechanism, and Fabrication Technologies: A Comprehensive Review. *Sensors* **2014**, *14*, 7881−7939.

(46) Grammatikos, S. A.; Ball, R. J.; Evernden, M.; Jones, R. G. Impedance spectroscopy as a tool for moisture uptake monitoring in construction composites during service. *Composites, Part A* **2018**, *105*, 108−117.

(47) Li, X.; Wang, X.; Zhao, Q.; Zhang, Y.; Zhou, Q. In Situ Representation of Soil/Sediment Conductivity Using Electrochemical Impedance Spectroscopy. *Sensors* **2016**, *16*, No. 625.

(48) Caballero, A. C.; Villegas, M.; Fernández, J. F.; Viviani, M.; Buscaglia, M. T.; Leoni, M. Effect of humidity on the electrical response of porous BaTiO3 ceramics. *J. Mater. Sci. Lett.* **1999**, *18*, 1297−1299.

(49) C-THERM. *Modified Transient Plane Source (MTPS)*, Theory of Operation. C-THERM, 2020.

(50) Bae, Y.-M.; Lee, Y.-H.; Kim, H.-S.; Lee, D.-J.; Kim, S. Y.; Kim, H.-D. Polyimide-polyurethane/urea block copolymers for highly sensitive humidity sensor with low hysteresis. *J. Appl. Polym. Sci.* **2017**, *134*, No. 11225.

(51) Bosch, P.; Fernández, A.; Salvador, E. F.; Corrales, T.; Catalina, F.; Peinado, C. Polyurethane-acrylate based films as humidity sensors. *Polymer* **2005**, *46*, 12200−12209.

(52) Currano, L. J.; Sage, F. C.; Hagedon, M.; Hamilton, L.; Patrone, J.; Gerasopoulos, K. Wearable Sensor System for Detection of Lactate in Sweat. *Sci. Rep.* **2018**, *8*, No. 15890.

(53) Farooqui, M. F.; Shamim, A. Low Cost Inkjet Printed Smart Bandage for Wireless Monitoring of Chronic Wounds. *Sci. Rep.* **2016**, *6*, No. 28949.

(54) Manjakkal, L.; Dang, W.; Yogeswaran, N.; Dahiya, R. Textile-Based Potentiometric Electrochemical pH Sensor for Wearable Applications. *Biosensors* **2019**, *9*, 14.

(55) Callewaert, C.; Buysschaert, B.; Vossen, E.; Fievez, V.; Van de Wiele, T.; Boon, N. Artificial sweat composition to grow and sustain a mixed human axillary microbiome. *J. Microbiol. Methods* **2014**, *103*, 6−8.

(56) Midander, K.; Julander, A.; Kettelarij, J.; Lidén, C. Testing in artificial sweat − Is less more? Comparison of metal release in two different artificial sweat solutions. *Regul. Toxicol. Pharmacol.* **2016**, *81*, 381−386.

(57) Ali, S.; Hassan, A.; Bae, J.; Lee, C. H.; Kim, J. All-Printed Differential Temperature Sensor for the Compensation of Bending Effects. *Langmuir* **2016**, *32*, 11432−11439.

(58) Molina-Lopez, F.; Vásquez Quintero, A.; Mattana, G.; Briand, D.; Rooij, N. Large-area compatible fabrication and encapsulation of inkjet-printed humidity sensors on flexible foils with integrated thermal compensation. *J. Micromech. Microeng.* **2013**, *23*, No. 025012.

(59) Nakata, S.; Arie, T.; Akita, S.; Takei, K. Wearable, Flexible, and Multifunctional Healthcare Device with an ISFET Chemical Sensor for Simultaneous Sweat pH and Skin Temperature Monitoring. *ACS Sens.* **2017**, *2*, 443−448.

(60) Schröter, A.; Rösen-Wolff, A.; Gerlach, G. In *Impedance Measurement of Wound Infection Status*, Proceedings SENSOR 2013. AMA Service GmbH, Ed.; 2013; pp 628−632.

(61) Furst, A. L.; Francis, M. B. Impedance-Based Detection of Bacteria. *Chem. Rev.* **2019**, *119*, 700−726.

(62) Derakhshandeh, H.; Kashaf, S. S.; Aghabaglou, F.; Ghanavati, I. O.; Tamayol, A. Smart Bandages: The Future of Wound Care. *Trends Biotechnol.* **2018**, *36*, 1259−1274.

(63) Mostafalu, P.; Tamayol, A.; Rahimi, R.; Ochoa, M.; Khalilpour, A.; Kiaee, G.; Yazdi, I. K.; Bagherifard, S.; Dokmeci, M. R.; Ziaie, B.;

Sonkusale, S. R.; Khademhosseini, A. Smart Bandage for Monitoring and Treatment of Chronic Wounds. *Small* **2018**, *14*, No. 1703509.

(64) Schröter, A.; Walther, A.; Fritzsche, K.; Kothe, J.; Rösen-Wolff, A.; Gerlach, G. Infection Monitoring in Wounds. *Proc. Chem.* **2012**, *6*, 175−183.

https://dx.doi.org/10.1021/acssensors.0c02037
ACS Sens. XXXX, XXX, XXX−XXX